Estimating tropical forest biomass with a combination of SAR image texture and Landsat TM data

Cutler, M. E. J.; Boyd, D. S.; Foody, G. M.; Vetrivel, Anand

Published in:
ISPRS Journal of Photogrammetry and Remote Sensing

DOI:
10.1016/j.isprsjprs.2012.03.011

Publication date:
2012

Document Version
Early version, also known as pre-print

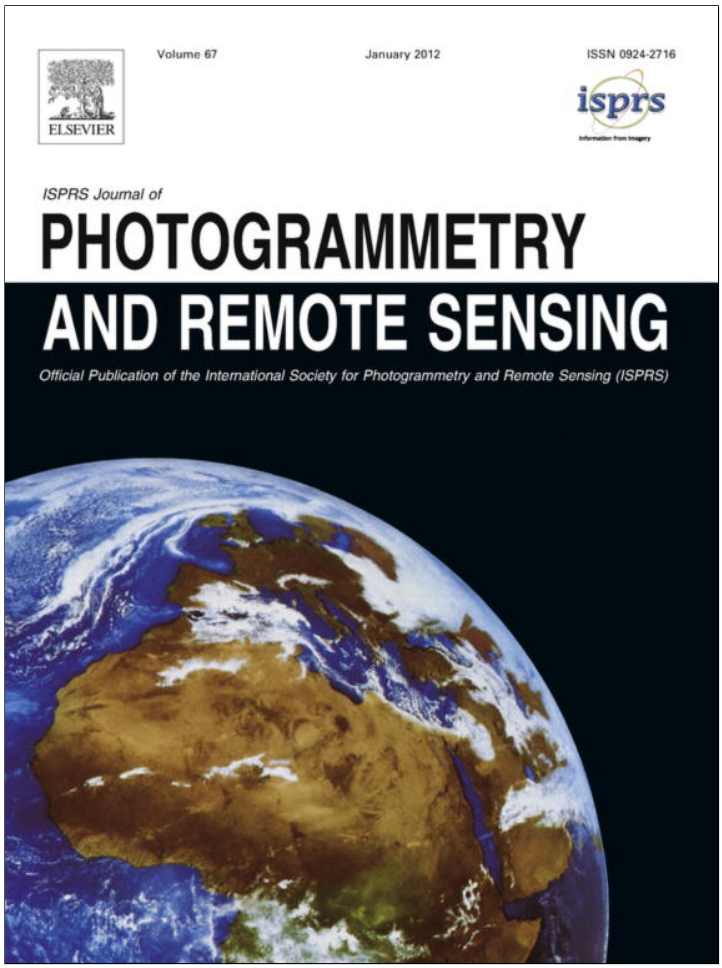

(This is a sample cover image for this issue. The actual cover is not yet available at this time.)

ISPRS Journal of Photogrammetry and Remote Sensing 70 (2012) 66–77

Contents lists available at SciVerse ScienceDirect

ISPRS Journal of Photogrammetry and Remote Sensing

journal homepage: www.elsevier.com/locate/isprsjprs

Estimating tropical forest biomass with a combination of SAR image texture and Landsat TM data: An assessment of predictions between regions

M.E.J. Cutler [a,*], D.S. Boyd [b], G.M. Foody [b], A. Vetrivel [a]

[a] School of the Environment, University of Dundee, Dundee DD1 4HN, UK
[b] School of Geography, University of Nottingham, Nottingham NG7 2RD, UK

ARTICLE INFO

Article history:
Received 30 June 2011
Received in revised form 6 January 2012
Accepted 27 March 2012

Keywords:
Biomass
SAR
Artificial neural network
Wavelets
Allometry

ABSTRACT

Quantifying the above ground biomass of tropical forests is critical for understanding the dynamics of carbon fluxes between terrestrial ecosystems and the atmosphere, as well as monitoring ecosystem responses to environmental change. Remote sensing remains an attractive tool for estimating tropical forest biomass but relationships and methods used at one site have not always proved applicable to other locations. This lack of a widely applicable general relationship limits the operational use of remote sensing as a method for biomass estimation, particularly in high biomass ecosystems. Here, multispectral Landsat TM and JERS-1 SAR data were used together to estimate tropical forest biomass at three separate geographical locations: Brazil, Malaysia and Thailand. Texture measures were derived from the JERS-1 SAR data using both wavelet analysis and Grey Level Co-occurrence Matrix methods, and coupled with multispectral data to provide inputs to artificial neural networks that were trained under four different training scenarios and validated using biomass measured from 144 field plots. When trained and tested with data collected from the same location, the addition of SAR texture to multispectral data showed strong correlations with above ground biomass ($r = 0.79$, 0.79 and 0.84 for Thailand, Malaysia and Brazil respectively). Also, when networks were trained and tested with data from all three sites, the strength of correlation ($r = 0.55$) was stronger than previously reported results from the same sites that used multispectral data only. Uncertainty in estimating AGB from different allometric equations was also tested but found to have little effect on the strength of the relationships observed. The results suggest that the inclusion of SAR texture with multispectral data can go someway towards providing relationships that are transferable across time and space, but that further work is required if satellite remote sensing is to provide robust and reliable methodologies for initiatives such as Reducing Emissions from Deforestation and Degradation (REDD+).

1. Introduction

The amount of carbon stored and sequestered by tropical forests represents one of the greatest uncertainties in understanding their role in the global carbon cycle (Houghton et al., 2000; Malhi, 2010). Quantifying this uncertainty demands methods that can accurately and precisely measure forest carbon dynamics (Brown, 2002), as well as map the geographic extent of forest cover and change over time. Previous attempts at carbon accounting have often been based upon estimating gross emissions, usually taking the form of mapping forest loss with little regard to replacement biomass and thus often overestimating the impact of avoided deforestation on carbon emissions to the atmosphere (UN-REDD, 2008). A more realistic assessment of carbon emissions to the atmosphere would be to estimate net emissions (i.e. carbon emission from deforestation and accumulation of carbon stocks from subsequent vegetation growth). A key driver for this is the United Nations Reducing Emissions from Deforestation and Degradation (UN-REDD+) programme, which explicitly states the need for the development of robust and replicable methods for net accounting of carbon emissions across large areas. Typically, governments and environmental scientists have relied upon official forest statistics to produce global assessments of forests but these suffer from poor temporal coverage, and variable definitions of forest degradation (Grainger, 2010). Estimating above ground forest biomass directly from satellite remote sensing is an attractive tool for deriving net carbon emissions estimates in a systematic and timely fashion, but its potential is yet to be realised operationally. One major problem with the remote sensing of biomass is that of generalizing or transferring knowledge and methods derived from

* Corresponding author. Tel.: +44 1382 385446; fax: +44 1382 388588.
E-mail address: m.e.j.cutler@dundee.ac.uk (M.E.J. Cutler).

0924-2716/$ - see front matter © 2012 International Society for Photogrammetry and Remote Sensing, Inc. (ISPRS). Published by Elsevier B.V. All rights reserved.
http://dx.doi.org/10.1016/j.isprsjprs.2012.03.011

remotely sensed data over time and space (Wilkinson, 1997; Nagendra, 2001; Woodcock et al., 2001).

Numerous studies have made use of remotely sensed data to study forested environments (Franklin et al., 2001; Boyd and Danson, 2005), but such data have not always been able to provide the specific environmental information required by the research and user communities. This is especially so in tropical environments where many have investigated the use of remotely sensed data to estimate tropical forest biomass but with varying degrees of success (e.g. Steininger, 2000; Foody et al., 2001, 2003; Castro et al., 2003; Wang and Qi, 2008; Hill et al., 2011). Even those attempts that have been successful have used methods that may not generalise accurately in time and space. For example, a relationship derived from the accurate prediction of biomass at one site or time may not yield accurate predictions when applied to images of another site and/or acquired at another time with either the same or a different sensor. This is a manifestation of the 'one time one place' approach identified by Woodcock (2002) as a common cause of uncertainty in the application of remotely sensed data to estimate forest biophysical properties. The elements of this problem are typically spatial (e.g. generalisation within an image or between imagery of different locations) and temporal (e.g. generalisation between images of one location acquired over a period of time) (Woodcock et al., 2001) and arise typically as a function of concerns with the remote sensing (e.g. consistent radiometric calibration) or ground conditions (e.g. spatial variation in forest structure). Such factors have been shown to significantly affect methods commonly used in previous studies, such as vegetation indices, which are highly sensitive to variation in topography, view angle and atmospheric conditions for example, and whose ability to predict above-ground biomass (AGB) of different tropical forest environments has been found wanting (Foody et al., 2001, 2003). Clearly, if remote sensing is to be a repeatable and consistent source of environmental information at regional scales then such issues must be addressed.

To address the problem of transferring a relationship geographically and develop a more consistently applicable approach to estimating tropical forest AGB with remotely sensed data, Foody et al. (2001, 2003) used an artificial neural network (ANN). This was trained with all six non-thermal Landsat TM wavebands and AGB measured in the field at three different tropical forest locations (one in S. America and two in S.E. Asia). The trained network was then tested to determine if a single ANN model could accurately estimate biomass at each site. When trained with data from a single site, the network was unable to accurately estimate AGB at the 'unseen' sites and performed only marginally better than a number of vegetation indices. More accurate predictions were obtained when the network was trained with data from all three sites ($r = 0.38$, significant at the 95% confidence level). The strongest correlation ($r = 0.49$, significant at the 99% confidence level) was observed when the network was trained with training data from all three sites and an additional variable identifying from which site the individual training samples were taken. Thus, a network trained with pixel values from six Landsat TM wavebands, corresponding AGB value and a label indicating the location of each sample, yielded a moderately strong correlation between estimated and observed AGB from all three sites.

Whilst such an approach appears promising, it is possible that an additional independent source of data that is able to discriminate between different forest locations by taking into account differing forest structure and other biophysical differences, could further improve the ability to estimate AGB at many sites concurrently and enhance spatial transferability (i.e. the transferring of predictive relationships between sites). Such independent data need to be widely available and should provide information in addition to that contained within multispectral data. This information could potentially be derived from active remote sensing systems which have been shown to be highly correlated with AGB in some environments (Brown, 2002; Lu, 2006; Mitchard et al., 2009).

LiDAR systems show particular promise in this respect (e.g. Hyde et al., 2006), but the availability of systematically acquired high-density LiDAR data for tropical regions remains very limited. Perhaps more useful at the present time is synthetic aperture radar (SAR). SAR data have been successfully used to estimate AGB in many forested environments, both by using the data to classify different forest types or by direct estimation. When classification-based methods have been used it has often been shown that texture information derived from SAR images can be especially useful in discriminating between different forest classes (e.g. Podest and Saatchi, 2002) as image texture contains information on the structural and geometric properties of forest canopies (DeGrandi et al., 2009). Direct estimation of AGB has been largely based upon the fact that SAR backscatter (σ^0) is sometimes strongly correlated with forest biomass, particularly in low-medium biomass forests and at lower frequencies (P- and L-band) (e.g. Le Toan et al., 1992; Luckman et al., 1997; Castel et al., 2002; Lucas et al., 2006a). Again, the addition of image texture measures has been shown to improve the accuracy with which biomass can be estimated in regenerating tropical forests (Kuplich et al., 2005). However, the use of SAR data to directly estimate forest AGB in tropical regions has well-known limitations, especially the problem of backscatter saturation at relatively low AGB. Previous studies have reported saturation at AGB of around 20 tha^{-1} for C-band and 40 tha^{-1} for L-band (Imhoff, 1995), although these may be extended through the use of backscatter ratios (Foody et al., 1997). The saturation effect is compounded by uncertainty in the relationships between AGB and SAR data resulting largely from a reliance on plot-based estimates of AGB that often fail to take into account variability in radar parameters, topography and forest structure (Luckman et al., 1997; Lucas et al., 2006a,b). It is likely that such issues have restricted investigation into the use of SAR data to estimate tropical biomass previously.

Several studies have investigated the integration of SAR and multispectral remotely sensed data for the estimation of forest biophysical properties. These have tended to employ a combination of optical and SAR data to aid discrimination of different vegetation and forest classes, from which typical AGB values for each class can be aggregated with respect to the entire classified area (e.g. Amini and Sumantyo, 2009). Another form of integration is to use SAR data as an extra variable (alongside multispectral wavebands and/or vegetation indices) in multivariate regression models. For example, Rauste (2005) used a combination of JERS-1 SAR backscatter and Landsat TM data to directly estimate stem volume of forests in Finland. This resulted in a slight increase in the accuracy of stem volume estimation compared to when SAR data alone were used (r increased from 0.85 to 0.89). As complementary data to multispectral Landsat TM imagery, therefore, the synergistic use of SAR and multispectral data for estimating AGB appears promising and deserves further attention (Lu, 2006).

Testing the spatial transferability of predictive relationships between remotely sensed data and AGB has received little attention to date. Mitchard et al. (2009) showed that a relationship derived between AGB and L-band backscatter was successful in estimating AGB in four different savannah and low biomass tropical forest environments in Africa. In high biomass tropical forests Foody et al. (2003) demonstrated that whilst AGB could be estimated at single sites reasonably well, poor accuracies were observed when relationships were used to estimate AGB at other sites. Whilst both the above studies used single source remotely sensed data, the aim of this paper is to investigate whether a combination of widely available multispectral (Landsat TM) and L-band SAR (JERS-1) backscatter and image texture measures can be used to improve

the spatial transferability of predictive relationships at three high-biomass tropical forest sites, as opposed to using multispectral data on their own.

2. Test sites and data

To test whether a combination of SAR and multispectral data could estimate AGB at different tropical forest locations empirical relationships were derived between ground estimates of AGB and the remotely sensed data. Forest plots were located at three different test sites, located near Manaus in Brazil (2° 28′ S, 59° 58′ W, Danum Valley Field Centre in Borneo, Malaysia, (4° 50′ N, 117° 45′ E) and part of the Khun Khong catchment in north-west Thailand (19° 31′ N, 98° 48′ E). All sites are located in the moist zone tropical forest region but differ in terms of tree species present, biophysical properties and AGB. For each site, JERS-1 SAR, Landsat TM and field survey data were acquired as close together as was practicable to facilitate meaningful comparisons (Table 1).

Twenty-two forest plots were located to the north and north-east of Manaus within the INPA and Smithsonian Institutes Biological and Forest Fragments Project (BDFFP) study area, with a further five established in the Ducke and Elger reserves (Lucas et al., 2002). Tree biophysical data were collected in 1993 and 1995 from rectangular plots of 100 × 10 m (0.1 ha), except for one plot that measured 20 × 15 m. For every tree within each plot that had a diameter at breast height (dbh cm) >3 cm, the tree species, dbh and height (m) (if possible) were recorded. The total above ground biomass (t ha^{-1}) of each tree was estimated using observations of dbh, height and the specific density of the wood (S, g cm^{-3}), when known, using the appropriate moist life zone allometric equation provided by Brown et al. (1989). Further details regarding these data may be found in Lucas et al. (2002).

A different sampling scheme was adopted for locating and sampling plots in both Thailand and Malaysia. Here, the dbh of all trees with a dbh > 10 cm within a circular plot with a radius of 12.62 m (0.05 ha) was measured (Pelz, 2000). Species and tree height (where possible) were also recorded, with total AGB again determined using appropriate moist life zone allometric equations (Brown, 1997) (Table 6).

A total of 52 plots were located within the lowland dipterocarp forests surrounding the Danum Valley Field Centre in northeastern Borneo, with observations made during field surveys in early 1997 (Foody et al., 2001). The region contains forest areas that have been logged at different times and intensities, as well as reserves of unlogged primary forest. A more complete description of the Borneo forest characteristics may be found in Newbery et al. (1992). Forest plots were located by segmenting the area into strata defined by past land use, with the date of logging activity or preservation status used as discriminating attributes. Five sample plots were located randomly within each stratum, except for one region in which two additional plots were also established.

The data from Thailand relate to forest plantations located within the Khun Khong Watershed Management Unit, approximately 100 km northwest of Chiang Mai. The majority of the 65 plots were located in stands of *Pinus kesiya* of different ages (32, 28, 25 and 19 years at the time of sampling in 1997), with the remainder in an area of tropical deciduous forest. A systematic sampling scheme was used to determine the location of each plot and positioned with the aid of a GPS. Further details relating to the collection of the ground data at all sites may be found in Foody et al. (2003), who used the same field data to estimate forest biomass with Landsat TM only.

3. Data processing

All remotely sensed data for each site were processed in the same way, before then being used to estimate AGB.

3.1. Remotely sensed data pre-processing

The Landsat TM data were radiometrically calibrated to top of the atmosphere radiance using post-launch calibration coefficients (Chavez, 1989) before then being atmospherically corrected using a modified dark object subtraction technique (Chavez, 1996). All images were then geometrically corrected using a first order polynomial function and 11 ground control points (GCPs) for the Malaysian image, 10 GCPs for the Thailand image and 20 for the Brazil image. This resulted in RMS errors of 18 m, 28 m and 14 m for the Malaysian, Thailand and Brazil images respectively. Finally, the images relating to Malaysia and Thailand were then topographically corrected according to the method presented by Ekstrand (1996) and using Digital Elevation Models (DEMs) for each site. Both DEMs were derived by digitising contours from 1:50,000 scale topographic maps and resampled to a spatial resolution of 30 m. As the Brazil test site was essentially flat then no topographic correction was required. A full description of all the pre-processing steps applied to the Landsat TM data can be found in Foody et al. (2003).

The JERS-1 SAR images were obtained from NASDA (level 2.1) and with a pixel spacing of 12.5 m. Each image was radiometrically calibrated to backscatter coefficients (σ^0) using the conversion equation provided by Shimada (2002). Both the Malaysian and Thailand sites showed some variation in backscatter due to terrain effects, both sites being located in areas of moderate relief and with some steep slopes. To account for this a terrain correction was applied to these two images only, similar to the Landsat TM data processing; as the site in Brazil is relatively flat no correction for terrain effects was applied. The DEMs that were used to topographically correct the Landsat TM images were used to derive slope and aspect, which in turn was used to calculate the local incidence angle for every pixel in the JERS-1 SAR images according to the method detailed by Sun et al. (2002). Radiometric distortions due to terrain effects were then corrected according to the equation outlined by Kellndorfer et al. (1998), which has previously been used by Sun et al. (2002) to estimate biomass with SIR-C data.

All JERS-1 SAR images were supplied already geo-referenced, although further correction was required for a more precise registration between the SAR and Landsat TM data. This was completed by selecting GCPs in both the multispectral and SAR images of each site and a 1st order polynomial transformation, with nearest neighbour resampling applied, but retaining the 12.5 m pixel size. All three sites were corrected to an estimated RMS error of less than one Landsat TM pixel (30 m) and subsequent visual inspection

Table 1
Ground and remotely sensed data sets.

Site	Field survey	Landsat TM (all six non-thermal wavebands)	JERS-1 (L-band)	Number of plots measured in the field
Brazil	July/August 1993 & 95	Landsat 4 July 1992	December 1995	27
Thailand	December 1997	Landsat 5 January 1997	March 1997	65
Malaysia	November & December 1996	Landsat 5 March 1997	December 1996	52

confirmed close agreement between the multispectral and SAR datasets.

3.2. SAR image texture

Image texture can provide information relating to the structural and geometric properties of forests (DeGrandi et al., 2009), which in itself may be correlated with AGB or be useful in discriminating between different forest types (Podest and Saatchi, 2002). Extracting image texture is commonly done using statistical and/or signal-processing methods (e.g. wavelet analysis). Here, both methods were used to obtain measures of image texture as additional variables to be combined with multispectral data for training artificial neural networks to estimate AGB on their own, and in combination with the Landsat TM data.

The Grey Level Co-occurrence Matrix (GLCM) is a statistically-based method of obtaining textural information from remotely sensed imagery of all types. It has been widely used for a variety of applications, including deriving estimates of biomass change in regenerating tropical forests (Kuplich et al., 2005). The GLCM is computed from a relative displacement vector (d, θ), which is based on the spatial distribution of grey level pairs of pixels separated by a distance (d) in a particular direction (θ). From this information, a number of textural measurements can be derived (Haralick, 1979). In this case the texture measures Entropy, Variance, Contrast, Dissimilarity, Homogeneity, Correlation, Second Moment and Energy were used, all of which have been shown to be useful in discriminating between tropical forest types (Podest and Saatchi, 2002). A detailed description of each texture measure can be found in Haralick (1979). Eight image texture measures were extracted from the GLCM for each location in the image where field data had been collected (Fig. 1). Selecting an appropriate window size for texture analysis is critical, as small window sizes often exaggerate differences, while large window sizes cannot effectively extract texture due to smoothing (Lu and Batistella, 2005). Rather than deciding upon a particular window size to generate texture measures in advance, all eight texture measures were generated for a range of window sizes from 3×3 pixels to 13×13 pixels. Texture was then derived for four commonly used directions within the window (45°, 90°, 135° and 0°), with the central pixel value derived from integrating all four values. To reduce computational effort the GLCM matrix was constructed using a 64 grey level quantisation, since high image quantization levels can generate sparse GLCMs, which may compromise the accuracy of the probability estimates for GLCM and, thus, any derived texture measures (Bijlsma, 1993).

Wavelet analysis is becoming more frequently used to derive texture information from SAR data. A discrete wavelet transform (DWT) decomposes images into different frequency components by applying a scaling function (low pass filter) and wavelet function (high pass filter). The original image can be decomposed into four frequency component images: approximation (low frequency information), and details (high frequency information) in three different directions (horizontal, vertical and diagonal). Further information and a mathematical basis for wavelet transformation is described by Daubechies (1991), whilst examples of their application to SAR image texture analysis are given in DeGrandi et al. (2009) and Simard et al., 1998 (2000). Commonly in a DWT filter bank design there is a decimation function after the data have been filtered, however in this case, to preserve the image size at every processing stage, a discrete wavelet frame transform (DWFT) was used which omits the decimation function. This decomposition process can be repeated to generate further levels of decomposition in which the approximation component is further decomposed into many frequency components. Three levels of Coiflet family wavelet decomposition were analysed and their corresponding scaling and wavelet coefficients are given in Table 2.

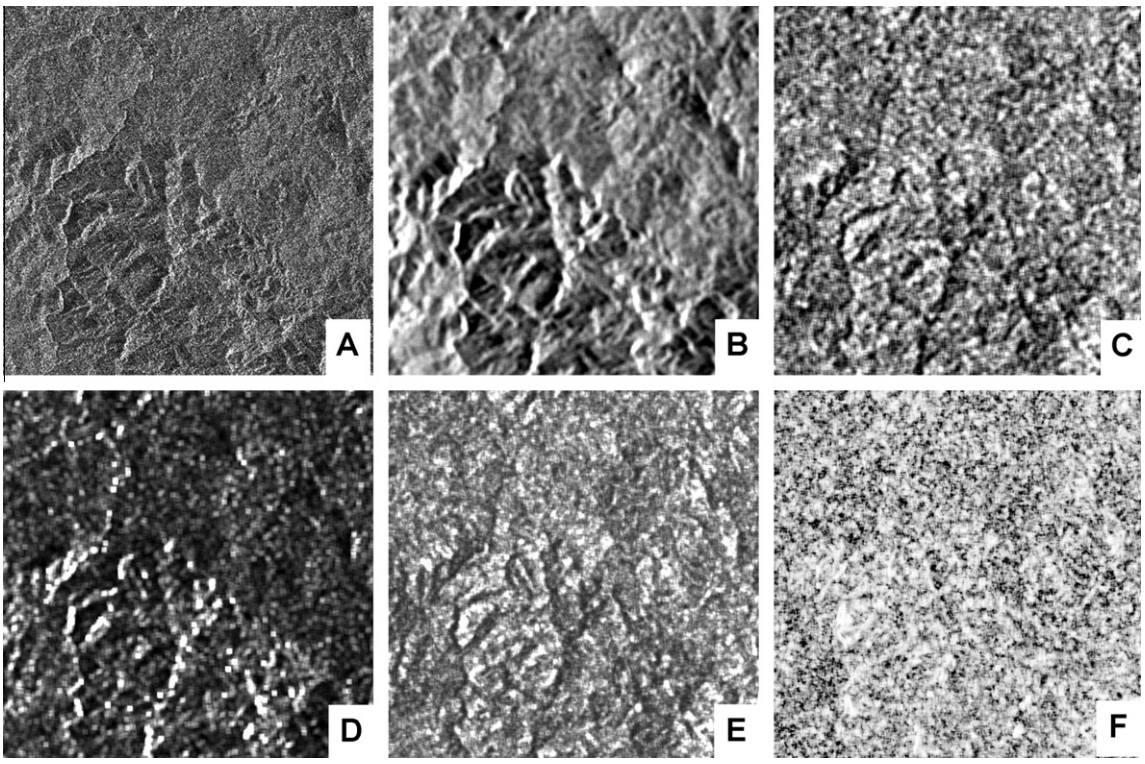

Fig. 1. Example JERS-1 SAR backscatter and GLCM-derived texture images (7×7 window) for the Malaysian site: (A) raw backscatter, (B) energy, (C) homogeneity, (D) contrast, (E) second moment, and (F) contrast.

Table 2
Scaling and wavelet coefficients for the three levels of Coiflet wavelet decomposition.

Coif1		Coif2		Coif3	
Scaling coefficient	Wavelet coefficient	Scaling coefficient	Wavelet coefficient	Scaling coefficient	Wavelet coefficient
−0.01565	−0.07273	−0.00072	0.01638	−0.000034	−0.003793
−0.07273	−0.33789	−0.00182	0.04146	−0.000070	−0.007782
0.38486	0.85257	0.00561	−0.06737	0.000467	0.023452
0.85255	−0.38486	0.02368	−0.38611	0.001117	0.065771
0.33789	−0.07273	−0.05943	0.81272	−0.002574	−0.061123
−0.07273	0.01565	−0.07648	−0.41700	−0.009007	−0.405176
		0.41700	−0.07648	0.015880	0.793777
		0.81272	0.05943	0.034555	−0.428483
		0.38611	0.02368	−0.082301	−0.071799
		−0.06737	−0.00561	−0.071799	0.082301
		−0.04146	−0.00182	0.428483	0.034555
		0.01638	0.00072	0.793777	−0.015880
				0.405176	−0.009007
				−0.061123	0.002574
				−0.065771	0.001117
				0.023452	−0.000467
				0.007782	−0.000070
				−0.003794	0.000034

3.3. Biomass estimation

At each location, the pixel containing a sample plot was identified and the SAR texture and backscatter information, along with reflectance in all 6 non-thermal Landsat TM wavebands extracted for the analyses. In total, 144 plots were surveyed in the field, but radar shadow precluded the use of 2 plots, leaving 142 for the analysis of SAR data only. Cloud contamination degraded the Landsat TM data by a further 48 plots, leaving 94 suitable for the combined SAR and Landsat TM analyses.

The most common method for estimating biophysical properties with remotely sensed data has been the use of vegetation indices. Typically, these have been used to generate some form of statistical relationship between the index and the biophysical variable of interest, before then deriving a predictive model based upon regression analyses. However, previous work has determined that this approach yielded inaccurate estimates at the three tropical forest sites used here and that the relationships were not transferable between sites (Foody et al., 2001, 2003). This is partly due to well known limitations of vegetation indices in high LAI environments (such as saturation) and partly to the problems of satisfying underlying assumptions of standard statistical regression analyses, such as data independence, distribution, absence of noise etc. Artificial neural networks, however, make no assumptions regarding the distribution and independence of input data and can still generalise effectively even when training data contain noise (Bishop, 1995). As such they may be used as an alternative to multivariate regression analysis, with an added benefit of making use of all spectral information present within multispectral data, as opposed to a limited number of wavebands when computing a vegetation index. Promising results have already been reported for the tropical forest sites used in this study using two feed forward neural network types: Multi-layer Perceptron (MLP) and Radial Basis Function (RBF) (Foody et al., 2001, 2003). Here, both types of ANN were used with various combinations of architectures and inputs evaluated. A software package that allows the testing of many networks with varying numbers of hidden units and layers which removes the often subjective process of the user deciding upon network architecture. For all networks the learning and momentum rates were set to the default values (0.3 and 0.1 respectively). The effects of varying these parameters was not investigated here, but clearly defining the optimum set of ANN parameters would be of significant value for wider application of this work. In all cases, the results reported here are for the network that showed the strongest correlation between the input training and testing datasets.

Above ground biomass was estimated using neural networks under four separate estimation scenarios. The first three scenarios used only the SAR texture and backscatter data to directly estimate AGB, whilst the fourth scenario investigated the use of combined SAR (texture) and Landsat TM data. The use of Landsat TM data on their own to estimate AGB has been reported previously (Foody et al., 2001, 2003) and whilst the raw field and Landat TM data are the same, it is important to note that the training and testing samples described below were generated randomly from the available SAR and multispectral data, and so will differ from the previous research. The results from each scenario were compared based upon the strength of the correlations between the observed and predicted AGB. The significance (95% confidence level) of any increase in strength of correlation between these and previously published results were tested using Fishers r to z transformation.

Table 3
Summary of the data used for training and testing ANNs in each of the different AGB estimation scenarios.

Scenario	Remotely sensed input data	No. of samples used in training	Trained with data from	No. of samples used in testing	Tested with data from
1	SAR backscatter and texture	18	Brazil	9	Brazil
		42	Thailand	21	Thailand
		34	Malaysia	18	Malaysia
2	SAR backscatter and texture	18	Brazil	39	Malaysia & Thailand
		42	Malaysia	30	Brazil & Thailand
		34	Thailand	27	Malaysia and Brazil
3	SAR backscatter and texture	94	Malaysia, Thailand & Brazil	48	Malaysia, Thailand & Brazil
4	SAR texture and Landsat TM	60	Malaysia, Thailand & Brazil	34	Malaysia, Thailand & Brazil

In the first scenario, neural networks were trained with samples obtained at one site (e.g. Thailand) and then tested with different samples from that same site to test whether there was a relationship between AGB and SAR backscatter and image texture at each site individually (analogous to the 'one time one place' approach). In each case, the data were divided randomly into two independent samples. One comprised data used to train the neural networks to develop an invertible relationship between forest biomass and the remotely sensed response, whilst the other contained the remaining data for that site which were used to evaluate the accuracy of the AGB estimates derived from the neural networks. For Brazil 18 samples were used for training and 9 for testing, for Thailand 42 were used for training and 21 for testing, and for Malaysia the training dataset comprised 34 samples, with 18 in the testing dataset.

In the second estimation scenario neural networks were again trained with data from a single site. However, in this case the neural networks that showed the strongest correlation with AGB in scenario 1 were now tested with data from sites other than which they were trained to evaluate the accuracy with which AGB at other sites could be estimated. For example, a network trained with data from Brazil was then tested with respect to its ability to estimate AGB in Malaysia and Thailand. Again, the data were divided into training data from a single site ($n = 18$, 42 and 34 for Brazil, Thailand and Malaysia respectively) whilst the testing data comprised the remaining samples from each site individually.

A third training scenario trained and tested the neural networks with data from all three sites. Here the training dataset comprised a total of 94 samples, randomly drawn from all three areas, with the remaining 48 samples making up the testing dataset.

In all three scenarios described above AGB was estimated firstly with backscatter values only, followed by all combinations of the eight GLCM-derived texture measures, and finally using the wavelet texture measures, again in combinations of all three levels of decomposition. It is important to note that there is likely to be a high degree of co-correlation between some of the GLCM and wavelet texture measures. By presenting different combinations of these inputs to the networks (i.e. not all measures were presented to every network) then the potentially negative effects of possible co-correlation is reduced, although this does increase processing time. The optimum selection of texture measures is clearly an important aspect of the wider application of this method and is the subject of further research.

The final estimation scenario involved training and testing ANNs with a combination of Landsat TM and SAR texture (GLCM) data drawn from all three sites. Corresponding pixel values from the texture and multispectral data were extracted for the 94 plots unaffected by cloud and radar shadow, before being randomly split into a training dataset of 60 and a testing dataset of 34 independent samples.

4. Results

Multiple individual ANNs were created in each of the four training scenarios, with each individual network varying in their network architecture, type and data used as inputs (although learning and momentum rates were kept constant throughout). Results are reported in all cases from the network that showed the strongest correlation with the testing data.

4.1. Scenario 1: training and testing ANNs with SAR texture data from the same site only

The JERS-1 SAR backscatter data on their own were weakly correlated with AGB, with correlation coefficients of $r = 0.23$ (Malaysia), $r = 0.05$ (Thailand) and $r = 0.16$ (Brazil), all insignificant at the 95% confidence level. Such weak relationships were not unexpected given the widely documented saturation of SAR backscatter data at high AGB, particularly in high biomass tropical forests (Imhoff, 1995; Lucas et al., 2006b).

There were strong correlations between the GLCM-derived image texture values and AGB when the neural networks were trained and tested with data from the same site, although there was considerable variability depending upon the window sizes used (Table 4). Networks trained with window sizes of 7×7 pixels all produced the strongest correlations between AGB values in the testing data and that predicted by the neural networks for all three sites ($r = 0.82$, 0.79 and 0.83 for Brazil, Malaysia and Thailand respectively). However, in each case the networks with the

Table 4
Correlation coefficients observed for the relationships between AGB of the testing set and that predicted by neural networks trained with varying sets of GLCM-derived SAR texture. Only those networks that showed the strongest correlation between training and testing data from the same site are presented (shown in bold type), along with the correlation coefficient when the same networks were used to predict AGB at different sites. The architecture of each neural network is indicated in the form of input: hidden: output units. The GLCM-derived texture measures are 1 energy, 2 variance, 3 homogeneity, 4 contrast, 5 dissimilarity, 6 entropy, 7 second moment, 8 correlation.

ANN type and architecture	Window size	Training site	Correlation coefficients for each testing site			GLCM texture variables used as inputs to ANN
			Brazil	Malaysia	Thailand	
MLP 7:4:1	3	Brazil	**0.48**	0.21	−0.13	1–7
MLP 3:4:1	5		**0.60**	0.32	−0.22	2,4,6
RBF 2:5:1	7		**0.82**	0.74	0.43	3,4
RBF 3:2:1	9		**0.81**	−0.38	−0.80	3,4,6
MLP 4:7:1	11		**0.83**	−0.44	−0.59	1,2,3,5
MLP 6:8:1	13		**0.84**	0.19	0.03	2,3,4,5,6,8
RBF 7:1:1	3	Malaysia	0.01	**0.40**	−0.27	2–8
MLP 5:8:1	5		-0.03	**0.43**	−0.23	1,2,3,4,6
RBF 7:3:1	7		0.76	**0.79**	0.23	1–4,6,7,8
MLP 4:7:1	9		0.20	**0.74**	−0.04	1,2,5,7
MLP 3:5:1	11		0.31	**0.48**	−0.51	1,3,7
RBF 8:10:1	13		0.09	**0.41**	0.17	1–8
MLP 8:6:1	3	Thailand	−0.41	0.15	**0.49**	1–8
MLP 3:3:1	5		0.03	0.37	**0.81**	1,2,3
MLP 5:9:1	7		0.13	−0.47	**0.83**	1,2,3,4,8
MLP 5:7:1	9		0.37	0.51	**0.78**	1,3,4,7,8
MLP 3:5:1	11		−0.51	0.01	**0.57**	2,3,4
RBF 5:6:1	13		0.34	0.22	**0.70**	3,4,5,7,8

strongest relationship between the remotely sensed data and AGB varied with respect to type, architecture and combination of texture measures used to train them. Similar results were also observed when networks were trained with Coiflet wavelet coefficients (Table 5). In general, Coiflet 3 produced the most consistent results in terms of strength of correlation at all sites individually ($r = 0.76$, 0.78 and 0.64 for Brazil, Malaysia and Thailand respectively), although this varied markedly with the degree of decomposition between sites, illustrating that it is difficult to define a single wavelet-derived texture measure that would be uniquely applicable at all three sites. This was tested further in scenario 2.

4.2. Scenario 2: training ANNs with SAR texture data from one site and applying that to other sites

The neural networks that exhibited the strongest relationship between the input data and AGB when trained and tested with data from the same site, were then evaluated with respect to their ability to estimate AGB at the two other sites (i.e. sites not used in training) (Tables 4 and 5). As in scenario 1, networks trained with backscatter data only from one site showed weak correlations when applied to other sites. More encouragingly, networks trained with GLCM-derived texture measures showed some degree of transferability, particularly when a 7×7 pixel window was used. Here, networks trained with samples from Brazil also showed a strong correlation when tested with data from Malaysia (e.g. $r = 0.74$ for MLP with 2 input units: 5 hidden: 1 output) and *vice versa*. However, weaker relationships were noted when applied to data from Thailand ($r = 0.43$) (Table 4). It should also be noted that there was little consistency in the architecture of the best performing networks and combinations of texture measures as inputs.

Similar results were observed when networks were trained with Coiflet wavelet inputs from one site and tested against samples from other sites (Table 5). Here though, the consistency of the relationships observed between the Brazilian and Malaysian data were less pronounced than the GLCM texture measures. For example, when trained and tested with data from Brazil ($r = 0.78$), the same network applied to Malaysia data produced only a moderate correlation ($r = 0.61$) (MLP with 4:8:1 units, Coiflet 1). It is interesting to note, however, that the horizontal component of the Coiflet wavelet was more often included as an input variable in the networks with the strongest correlation with AGB than any other wavelet texture measures. Whilst no further statistical analysis of the sensitivity of networks to the various input variables is presented here, determining why this component was most frequently associated with strongly performing networks and defining the most suitable texture measures for estimating AGB warrants further investigation.

4.3. Scenario 3: training and testing ANNs with SAR texture data drawn from all 3 sites

Previous work has suggested that a neural network trained with remotely sensed data from a single site is unlikely to be able to estimate AGB with any great accuracy when tested with data from a different site (Foody et al., 2003). Whilst the results from scenario 2 show that networks were sometimes able to predict biomass at other sites, the lack of consistency in estimating AGB across all sites suggests that further investigation is required. Therefore, a further set of neural networks were trained with GLCM-derived SAR texture measures, with samples randomly selected from all three sites (Malaysia, Thailand and Brail) and subsequently tested with independent (unseen) cases, again drawn from all three forest

Table 5
Correlation coefficients observed for the relationships between AGB of the testing set and that predicted by neural networks trained with Coiflet wavelet coefficients at varying degrees of decomposition and input variables. Only those networks that showed the strongest correlation between training and testing data from the same site are presented (shown in bold type), along with the correlation coefficient when the same networks were used to predict AGB at different sites. The architecture of each neural network is indicated in the form of input: hidden: output units. The input Coiflet texture variables were 1 approximation, 2 horizontal, 3 vertical and 4 detail.

ANN type and architecture	Wavelet family	Level of de-composition	Training site	Correlation coefficients for each testing site			Coiflet texture variables used as inputs to ANN
				Brazil	Malaysia	Thailand	
MLP 4:8:1	Coif1	1	Brazil	**0.78**	0.61	−0.19	1,2,3,4
RBF 2:5:1	Coif1	2		**0.46**	0.25	−0.43	1,2
MLP 2:5:1	Coif1	3		**0.63**	0.59	0.34	2,3
MLP 4:7:1	Coif2	1		**0.71**	0.40	0.20	1,2,3,4
MLP 3:5:1	Coif2	2		**0.51**	0.54	0.17	2,3,4
RBF 2:2:1	Coif2	3		**0.64**	−0.21	0.07	2,3
MLP 4:7:1	Coif3	1		**0.65**	0.23	0.64	1,2,3,4
MLP 3:3:1	Coif3	2		**0.71**	0.14	0.17	2,3,4
MLP 2:4:1	Coif3	3		**0.76**	−0.61	−0.47	2,3
MLP 2:3:1	Coif1	1	Malaysia	−0.49	**0.54**	0.42	2,3
MLP 2:3:1	Coif1	2		0.20	**0.60**	−0.33	1,2
MLP 2:3:1	Coif1	3		0.47	**0.67**	0.28	2,3
MLP 4:7:1	Coif2	1		0.26	**0.44**	−0.59	1,2,3,4
MLP 2:3:1	Coif 2	2		−0.38	**0.34**	−0.49	2,3
MLP 2:7:1	Coif2	3		−0.59	**0.35**	−0.01	2,3
MLP 4:7:1	Coif3	1		0.62	**0.70**	0.51	1,2,3,4
MLP 2:3:1	Coif3	2		−0.38	**0.74**	−0.49	2,3
MLP 2:5:1	Coif3	3		−0.50	**0.78**	−0.14	2,3
MLP 2:7:1	Coif1	1	Thailand	0.50	0.45	**0.62**	2,3
MLP 2:3:1	Coif1	2		−0.67	−0.20	**0.23**	2,3
MLP 2:3:1	Coif1	3		0.01	−0.48	**0.60**	2,3
MLP 3:5:1	Coif2	1		0.22	0.08	**0.51**	1,3,4
MLP 2:3:1	Coif2	2		−0.39	0.01	**0.47**	1,2
MLP 2:3:1	Coif2	3		0.08	−0.29	**0.42**	2,3
MLP 3:3:1	Coif3	1		0.55	0.42	**0.64**	1,3,4
MLP 2:3:1	Coif3	2		−0.29	0.11	**0.50**	1,2
MLP 2:5:1	Coif3	3		0.03	−0.39	**0.44**	2,3

Table 6
Summary of correlation coefficients observed for the relationships between different combinations of input data and AGB, predicted by neural networks trained and tested with data drawn from all three sites (Malaysia, Brazil and Thailand).

Data combination	Correlation coefficient (r)
Landsat TM	0.38[a]
Landsat TM + country label	0.49[a] (0.68 when two outliers removed)
SAR image texture[b]	0.55
Landsat TM, SAR image texture[c]	0.77

[a] From Foody et al. (2003).
[b] MLP 3:5:1, trained using GLCM-derived texture measures homogeneity, contrast and dissimilarity.
[c] MLP 11:7:1, trained using all Landsat TM wavebands (except band 6) and GLCM texture measures energy, variance, homogeneity, contrast and dissimilarity.

sites. Informed by previous results, GLCM-textures were derived for a 7 × 7 pixel window only to minimise training time.

The ANN that showed the strongest relationship between actual and predicted AGB ($r = 0.53$, significant at the 95% confidence level) (Table 6, Fig. 2) was a MLP (4:5:1 units). The strength of the relationship compares well with relationships previously reported when a neural network was trained and tested with only Landsat TM data from the same three sites ($r = 0.38$) (Foody et al., 2003). However, it is clear from Fig. 2 that AGB is consistently underestimated, particularly for high-biomass plots.

4.4. Scenario 4: training and testing with SAR texture and Landsat TM data from all 3 sites

There was a strong positive relationship between the observed and predicted AGB when neural networks were trained and tested with Landsat TM and JERS-1 SAR GLCM-derived texture information from all sites ($r = 0.77$ significant at the 99% confidence level) (Fig. 3; Table 6). In particular, the underestimation of biomass noted in Fig. 2 when only SAR GLCM data were used is not so apparent here when Landsat TM data were included. This was also a stronger correlation coefficient than that observed when a network was previously trained and tested with Landsat TM data only ($r = 0.38$) and a combination of Landsat TM data plus a geographic label denoting which site training data came from ($r = 0.49$) (Foody et al., 2003). The difference in strength of correlations was assessed using Fishers r-to-z transformation. For the correlations using just the Landsat TM data only and the SAR texture measures only to estimate AGB there was a significant difference ($r = 0.38$ and 0.77 respectively, $z = 2.38$, $p < 0.05$). However, when the combined Landsat TM and SAR texture relationship ($r = 0.77$) was compared with those derived previously for the Landsat TM data plus a geographic label ($r = 0.49$), there were no significant differences ($z = 0.1.878$, $p = 0.0604$ and $z = 0.73$, $p = 0.4633$ respectively). It should be noted, however, that in both cases the sample size used in the testing datasets were relatively small ($n = 34$ and 31 respectively).

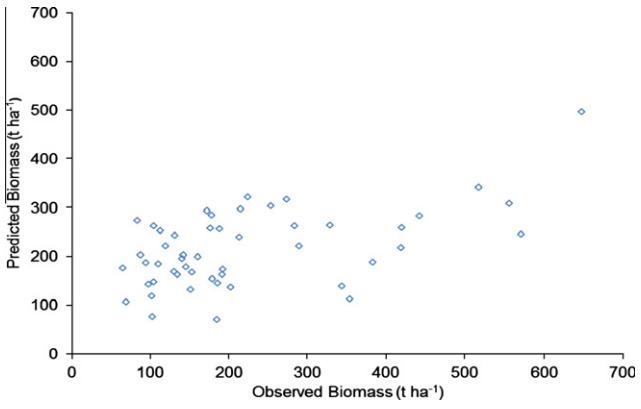

Fig. 2. Observed and predicted biomass from a network trained and tested with SAR GLCM texture from all sites ($r = 0.53$, statistically significant at the 99% confidence level, $n = 51$).

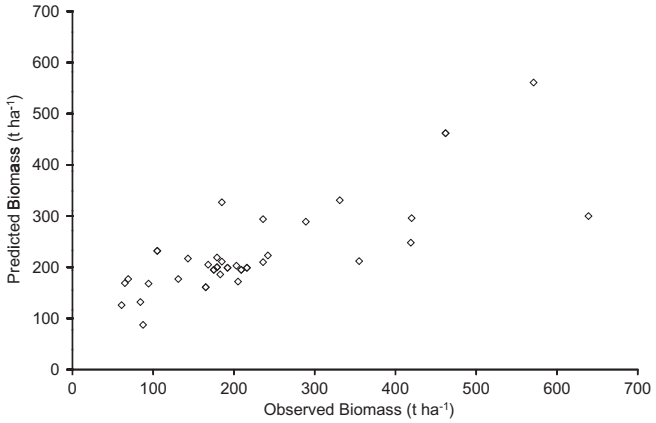

Fig. 3. Observed and predicted biomass from a network trained and tested with Landsat TM and JERS-1 SAR texture data from all sites ($r = 0.77$, statistically significant at the 99% confidence level, $n = 34$).

5. Discussion

5.1. SAR texture

The two independently derived measures of SAR image texture (wavelet and GLCM-based) were both highly correlated with AGB when neural networks were trained and tested with texture samples from the same sites only. In fact, the strength of the correlations observed are comparable to those reported previously (Foody et al., 2001, 2003), when neural networks were trained and tested with Landsat TM data only from the same sites ($r = 0.82$, 0.71 and 0.84 for Malaysia, Thailand and Brazil respectively). This demonstrates the considerable potential of using SAR image texture to estimate AGB at individual tropical forest sites. This potential has been highlighted before, with the addition of texture measures shown to increase the strength of relationships between SAR backscatter and AGB (e.g. Kuplich et al., 2005). However, a key difference between this work and previous studies is the fact that a number of texture measures are used in combination to train and test multiple neural networks, rather than selecting either a single measure of texture or using techniques such as stepwise multiple regression. The use of multiple neural networks, trained with combinations of image texture measures and window sizes, allows the user to make fewer decisions regarding these key inputs to the model, but rather select the 'best' performing network. The trade-off, however, is in processing time and the fact that this approach demands available data to be split into training and testing data. With ground data in tropical forests often difficult to obtain, this can lead to very small testing datasets from which firm statistical conclusions may be difficult to draw. However, the results suggest that given the often extensive cloud cover in tropical areas and the problematic effects of the atmosphere upon multispectral data, SAR texture may provide a means of obtaining information relating to AGB and carbon stocks on a more frequent basis than possible with optical sensors.

5.2. Spatial transferability of relationships

Whilst in general ANNs trained with data from one site showed a poor ability to estimate AGB at other sites, there was a discernible

pattern in that networks trained with samples from Brazil also showed a strong correlation when tested with data from Malaysia, and *vice versa* (Tables 4 and 5). This is largely attributable to the forest characteristics and properties at each of these two sites being more similar than the forest in Thailand. Both the Malaysian and Brazil sites are located in lowland tropical forest areas, both subjected to logging and with broadly similar canopy structures (but very different species assemblages). The site in Thailand, however, has forest more akin to the characteristics of montane tropical forest, with planted stands of *P. kesiya*. These functional similarities (between Brazil and Malaysia) and differences (with Thailand) help to explain why the relationships derived for Brazil and Malaysia are more applicable to each other than the Thailand forests. Whilst not providing a truly globally applicable relationship for all tropical forest regions, the use of SAR texture produced relationships with stronger correlations than when Landsat TM data only were analysed in a similar fashion (Foody et al., 2003) and suggest that generally applicable relationships may be possible for forests of similar functional types, although clearly more testing is required.

A further solution to increase the transferability of predictive relations between sites may be the incorporation of a geographic label, as demonstrated by Foody et al. (2003). However, an ANN trained with data that incorporates a geographical label is probably deriving a series of internal local, rather than global relationships although this is difficult to verify, i.e. the label divides the data into different geographical groups and separate relationships between the remotely sensed data and AGB derived, but within a single ANN. When such a network is used to estimate AGB from observations made outside of the area from which it has been trained, it is likely to perform poorly unless the new site observations fall within the bounds of these local relationships. Whether replacing a geographic label with forest information derived from an independent data source (e.g. SAR) provides a more representative global relationship (given that information relating to forest structure etc. is present) is quite likely, but requires further analysis.

The results presented here once again highlight the problem of transferring a predictive relationship between different locations. This is perhaps not a surprise given the numerous sources of uncertainty and error that could be included within the analysis. These sources may be categorised into uncertainty introduced through ground data collection, biomass estimation methods and image processing procedures.

5.3. Uncertainty in AGB estimation from field measurements

A major source of uncertainty in the estimation of tropical forest AGB is the lack of standard models for deriving AGB from direct tree measurements (Chave et al., 2005). The use of allometric regression models is common but many remain largely untested beyond their initial development (Brown et al., 1989). Previous studies have illustrated that large variation in stand level AGB estimates have been observed when different allometric equations are applied (e.g. Chave et al., 2005) although this does not appear to significantly affect estimates of the magnitude of tropical AGB change (Baker et al., 2004). However, to test whether variation in AGB estimation from field data had an impact upon remotely sensed estimates of AGB the field data were re-analysed and neural networks trained and tested using a 'new' set of biomass estimates and a combination of SAR texture and Landsat TM data.

As described in Section 2, the analysis presented thus far has been based upon AGB estimation using allometric equations given by Brown (1997) (Table 7). These were developed from tree measurements made across several tropical regions and from mixed species (so called 'pan-tropic' models). However, such models naturally generalise variation in AGB response to stem diameter, meaning that forest-type, regional or even species dependent models may well yield more accurate estimates of AGB (Chave et al., 2005; Basuki et al., 2009). Here, the tree biophysical data were used to estimate AGB a second time but using allometric equations that were either developed for specific species (e.g. *Dipterocarp*) or regions (e.g. Amazonia) (Table 7).

In Malaysia, AGB varied between allometric equations by up to 260 t ha^{-1}, representing a percentage difference of 50%, varying markedly in plots where biomass was high (Conservation Area and Water Catchment regions). In all cases, the pan-tropic equation of Brown (1997) produced much higher estimates of AGB than the *Dipterocarp* specific equation of Basuki et al. (2009), with those plots containing large trees (dbh > 30 cm) being particularly different. A similar pattern was observed in Brazil, with the pan-tropic equation again consistently producing higher estimates of AGB than the region specific allometric equations of Uhl et al. (1988). AGB estimates ranged between 13 and 239 t ha^{-1}, representing percentage differences of 8–60% respectively. The differences between AGB estimates in Thailand, however, were not uniformly distributed between the two sets of equations. For those plots dominated by *P. kesiya* the pan-tropic equations produced much

Table 7
Allometric equations used to estimate total above ground biomass and the regions to which they were applied.

Author and model	Applied to			
	Malaysia	Thailand		Brazil
		Pinus	Other species	
Brown et al. (1989), Brown (1997)				
$Y = \exp(-2.134 + 2.53\ln(D))$	•		•	•
Brown et al. (1989), Brown (1997)				
$lnY = -1.201 + 2.196\ln(D))$		•		
Basuki et al. (2009)				
$lnY = -1.201 + 2.196\ln(D)$	•			
Baishya and Barik (2011)				
$Y = 1.3503 - 3.4145(D) + 4.8678(D)^2 - 1.352(D)^3$		•		
Chambers et al. (2001)				
$\ln(Y_1) = -0.37 + 0.333\ln(D) + 0.933(\ln(D))^2 - 0.122(\ln(D))^3$			•	
Uhl et al. (1988)				
$\ln Y = -2.17 + 1.02\ln(D) + 0.39\ln(H)$				•

Where Y is Total Above Ground Biomass, D is Diameter at breast height and H is height.

Table 8
Correlation coefficients observed for the relationships between region-specific AGB and that predicted by neural networks trained with varying sets of GLCM-derived SAR texture. Only those networks that showed the strongest correlation between training and testing data from the same site are presented (shown in bold type), along with the correlation coefficient when the same networks were used to predict AGB at different sites. The architecture of each neural network and the GLCM-derived texture measures are as in Table 3.

ANN type and architecture	Training site	Correlation coefficients for each testing site			GLCM texture variables used as inputs to ANN
		Brazil	Malaysia	Thailand	
MLP 2:6:1	Brazil	**0.85**	0.70	0.57	3,4
RBF 2:4:1	Brazil	**0.78**	0.76	0.44	3,4
RBF 2:4:1	Malaysia	0.74	**0.81**	0.42	1,3,4,8
MLP 1:2:1	Thailand	0.49	0.45	**0.79**	3,
MLP 5:7:1	Thailand	0.53	0.49	**0.86**	1,3,4,7,8

higher estimates of AGB than when the plots were dominated by mixed species, where estimates of AGB were similar (0.5–74 t ha^{-1}, representing percentage differences of 0.5–27% respectively).

Using the same procedure described in training scenario 2, neural networks were initially trained with AGB and SAR GLCM-texture from each site individually, and then tested against data drawn from all three sites. The results (Table 8) indicated that the strength of the relationships between AGB and SAR GLCM were similar to those presented in Section 4.2. Strong correlations were observed when networks were trained and tested with data from the same site (r = 0.85, 0.81 and 0.86 for Brazil, Malaysia and Thailand respectively). Again similar to previous results, when networks trained with data from one site were presented with data from a different site weaker correlations were observed, although it is interesting to note that once again networks trained with data from Brazil were able to estimate AGB in Malaysia fairly well (r = 0.70) and *vice versa* (r = 0.74).

Subsequently, a neural network (MLP 11:11:1) was trained and tested using all SAR GLCM texture measures and all 6 Landsat TM wavebands (as per scenario 4). A strong correlation was observed (r = 0.72, significant at the 99% confidence level, n = 34), which again corresponds well with the output from Section 4.4 (r = 0.77).

The similarity between the strength of the relationships observed between the remotely sensed data and the two different estimates of AGB is largely unsurprising, with the relative differences in AGB between plots and locations largely maintained. What is interesting is that the region/species-specific allometric equations appear to produce AGB estimates that are more uniform, especially when plots include large trees. The use of an ANN to estimate AGB in this analysis may also ameliorate uncertainty in AGB estimation, as noise within the training and testing datasets is likely to be more tolerated than using a vegetation index or standard regression approach.

5.4. Other factors limiting transferability

Determining AGB in the field can introduce bias and error through variable sampling strategies, whilst data processing also represents a source of uncertainty. Foody et al. (2003) discuss these sources of error, particularly highlighting the pre-processing of Landsat TM data as a possible source. In addition, the extra image processing required to process and co-register the SAR data represents further opportunities for errors to be introduced, particularly with respect to the terrain correction of the JERS-1 SAR data. Ideally, different backscattering models are required for forests of different structure and terrain (Sun et al., 2002), but in this case they were assumed to be uniform. There was also a difference in time between the collection of the ground, Landsat TM and JERS-1 SAR data (Table 1), particularly with respect to Brazil. Whilst every effort was made to find suitable coincident data, a pragmatic rather than ideal approach was required, particularly given the problems of obtaining cloud free multispectral data of the tropics. The effects of this inconsistency on our results is uncertain, and whilst this could conceivably be addressed through the use of ecosystem simulation models of forest productivity, this would require further field validation and is beyond the scope of this paper.

Also, whilst measures of SAR texture show real promise in being used as inputs to estimate AGB at sites both individually and wider, in practice it remains difficult to identify the appropriate texture measures that will yield the strongest results for each site, with different combinations of texture measures, window sizes and levels of wavelet decomposition being included here in the strongest performing models, something which has also been highlighted by others (e.g. Lu and Batistella, 2005; Lu, 2006). Selecting the most appropriate texture measure and parameters may require analysis of the geostatistical properties (spatial dependence) of the image, for example, but requires further attention if generally applicable methods (both spatially and temporally) are to be proposed (Lu, 2006).

With respect to AGB estimation then the use of standard regression analysis makes certain assumptions regarding the distribution, independence and quality of the data being analysed. In many environmental datasets these assumptions are violated and point toward the use of non-parametric methods such as ANNs. However, a commonly cited limitation of the use of ANNs is that they are a so called 'grey box' method, which usually refers to the fact that there is limited information as to how the network arrived at a particular result. This means that, unlike more commonly used parametric methods (e.g. regression between vegetation indices and vegetation variables) the nature and form of the relationship between the input and output variables is not known. It is possible to analyse the weights within a trained network to provide some measure of the importance of input variables. For example, Foody et al. (2001) determined that Landsat TM waveband 1 was the most significant for estimating the biomass of tropical forests in Malaysia using an ANN. However, the interpretation of these data is often open to question with no explanation as to why a particular variable has a perceived increased importance within the ANN model over another. Clearly, further understanding of the spectral response of forest canopies at optical and microwave wavelengths is required and will be vital for understanding relationships observed and developing generally applicable methods for estimating tropical forest AGB at multiple sites concurrently. To this end, the application of new SAR sensor systems to this problem may well yield promising results. Of particular interest is the L-band radar sensor Advanced Land Observing Satellite (ALOS) Phased Array L-band Synthetic Aperture Radar (PALSAR) which has already been shown to provide widely applicable relationships between SAR backscatter and lower biomass woody vegetation at regional scales (Mitchard et al., 2009). The provision of cross-polarized data, in particular, may provide additional discriminatory variables and information for input to models of biomass estimation across different forest types.

6. Summary and conclusions

A key requirement in the construction of global knowledge in relation to tropical forests is that methods and relationships should be repeatable and applicable across different tropical forest types and locations. A common argument for the use of remote sensing to generate this knowledge is that it should be able to provide estimates of forest properties in a consistent manner, given the systematic way in which data are collected and potential for standard processing routines to be used. This suggests an ability to generalise in space and time, implying that it should be possible to successfully apply a predictive relation at times and locations other than for which it was developed. The results presented here show that combining independent observation data from SAR and multispectral sources may provide some degree of transferability, but also highlight problems in transferring predictive relations across space. The main results were:

- There was a number of strong relationships observed between SAR texture and AGB, whether that was texture derived using GLCM-based texture measures or wavelet analysis. The strength of these relationships when networks were trained and tested with data from the same site suggest that the use of SAR texture to estimate AGB in high biomass tropical forests is promising and warrants further investigation, especially given the advantages of SAR data collection in cloudy locations compared to multispectral systems.
- The accuracy of predictive relations, as described by their correlation with ground data, declined when applied to different regions, similar to the results observed when Landsat TM data only were investigated in the same three regions previously (Foody et al., 2003). However, there was some evidence for a degree of transferability when networks trained with data from Brazil were applied to sites in Malaysia, and *vice versa*. This suggests that for forests of similar functional types then the use of SAR texture information may again hold promise for providing generally applicable relationships.
- A neural network trained and tested on a combination of JERS-1 SAR texture and Landsat TM data drawn from all three regions provided the strongest correlation with AGB at all sites.
- Uncertainty in AGB estimation from field data was assessed by repeating some of the analyses with AGB derived from region-specific allometric equations. Whilst field-AGB varied by up to 60% between equations, the impact upon the strength of relationships between AGB and the remotely sensed data was minimal.

It is evident that further investigation is required if remote sensing is to reach its full potential as a source of information for developing robust, transparent, replicable and long-term monitoring systems that are demanded by programmes such as REDD.

Acknowledgements

The field and optical remotely sensed data for the Malaysian and Thailand test sites were acquired for the EU-funded INDFORSUS project (ER-BIC18T960102), while the field and optical data for the Brazilian test site were acquired through the NERC TIGER project (GST/02/604). We are grateful to all involved with these projects for their assistance and input. The acquisition and processing of the JERS-1 data was made possible as a result of financial assistance from the Carnegie Trust for the Universities of Scotland. This article benefited from involvement in the Royal Society's Southeast Asia Rainforest Research Programme. Finally we thank the anonymous reviewers of the manuscript for their helpful suggestions for improvement.

References

Amini, J., Sumantyo, J.T.S., 2009. Employing a method on SAR and optical images for forest biomass estimation. IEEE Transactions on Geoscience and Remote Sensing 47 (12), 4020–4026.

Baishya, R., Barik, S.K., 2011. Estimation of tree biomass, carbon pool and net primary production of an old growth *Pinus Kesiya* Royle ex. Gordon forest in North-eastern India. Annals of Forest Science 68 (4), 727–736.

Baker, T.R., Phillips, O.L., Malhi, Y., Almeida, S., Arroyo, L., Di Fiore, A., Erwin, T., Higuchi, N., Killeen, T.J., Laurance, S.G., Laurance, W.F., Lewis, S.L., Monteagudo, A., Neill, D.A., Vargas, P.N., Pitman, N.C.A., Natalino, J., Silva, M., Martinez, R.V., 2004. Increasing biomass in Amazonian forest plots. Philosophical Transactions of the Royal Society of London Series B 359, 381–407.

Basuki, T.M., van Laake, P.E., Skidmore, A.K., Hussin, Y.A., 2009. Allometric equations for estimating the above-ground biomass in tropical lowland *Dipterocarp* forests. Forest Ecology and Management 257 (8), 1684–1694.

Bijlsma, R.J., 1993. The characterisation of natural vegetation using first-order and texture measurements in digitized, color-infrared photography. International Journal of Remote Sensing 14 (8), 1547–1562.

Bishop, C.M., 1995. Neural networks for pattern recognition. Clarendon Press, Oxford.

Boyd, D.S., Danson, F.M., 2005. Satellite remote sensing of forest resources: three decades of research development. Progress in Physical Geography 29 (1), 1–26.

Brown, S., 1997. Estimating biomass and biomass change of tropical forests. FAO Forestry Paper, vol. 134. Rome, FAO.

Brown, S., 2002. Measuring carbon in forests: current status and future challenges. Environmental Pollution 116 (3), 363–372.

Brown, S., Gillespie, A.J.R., Lugo, A.E., 1989. Biomass estimation methods for tropical forest with application to forest inventory data. Forest Science 35 (4), 881–902.

Castel, T., Guerra, F., Caraglio, Y., Houllier, F., 2002. Retrieval biomass of a large Venezuelan pine plantation using JERS-1 SAR data. Analysis of forest structure impact on radar signature. Remote Sensing of Environment 79 (1), 30–41.

Castro, K.L., Sanchez-Azofeifa, G.A., Rivard, B., 2003. Monitoring secondary tropical forests using space-borne data: implications for Central America. International Journal of Remote Sensing 24, 1853–1894.

Chambers, J.Q., dos Santos, J., Ribeiro, R.J., Higuchi, N., 2001. Tree damage, allometric relationships, and aboveground net primary production in central Amazon forest. Forest Ecology Management 152 (1–3), 73–84.

Chave, J., Andalo, C., Brown, S., Cairns, M.A., Chambers, J.Q., Eamus, D., Fölster, H., Fromard, F., Higuchi, N., Kira, T., Lescure, J.-P., Nelson, B.W., Ogawa, H., Puig, H., Riéra, B., Yamakura, T., 2005. Tree allometry and improved estimation of carbon stocks and balance in tropical forests. Oecologia 145, 87–99.

Chavez, P.S., 1989. Radiometric calibration of Landsat Thematic Mapper multispectral images. Photogrammetric Engineering and Remote Sensing 55 (9), 1285–1294.

Chavez, P.S., 1996. Image-based atmospheric corrections: revised and improved. Photogrammetric Engineering and Remote Sensing 62 (9), 1025–1036.

Ekstrand, S., 1996. Landsat TM-based forest damage assessment: correction for topographic effects. Photogrammetric Engineering and Remote Sensing 62 (2), 151–161.

Daubechies, I., 1991. The wavelet transform: a method for time–frequency localization. In: Haykin S. (Ed.), Advances in Spectrum Analysis and Array Processing, vol. 1.

DeGrandi, G., Lucas, R.M., Kropacek, J., 2009. Analysis by wavelet frames of spatial statistics in SAR data for characterising structural properties of forests. IEEE Transactions on Geoscience and Remote Sensing 47 (2), 494–507.

Foody, G.M., Green, R.M., Lucas, R.M., Curran, P.J., Honzak, M., Do Amaral, I., 1997. Observations on the relationship between SIR-C radar backscatter and the biomass of regenerating tropical forests. International Journal of Remote Sensing 18 (3), 687–694.

Foody, G.M., Cutler, M.E.J., McMorrow, J., Pelz, D., Tangki, H., Boyd, D.S., Douglas, I., 2001. Mapping the biomass of Bornean tropical forest. Global Ecology and Biogeography 10 (4), 379–387.

Foody, G.M., Boyd, D.S., Cutler, M.E.J., 2003. Predictive relations of tropical forest biomass from Landsat TM data and their transferability between regions. Remote Sensing of Environment 85 (4), 463–474.

Franklin, S.E., Wulder, M.A., Gerylo, G.R., 2001. Texture analysis of IKONOS panchromatic data for Douglas fir forest age class separability in British Columbia. International Journal of Remote Sensing 22 (13), 2627–2632.

Grainger, A., 2010. Uncertainty in the construction of global knowledge or tropical forests. Progress in Physical Geography 34 (6), 811–844.

Haralick, R.M., 1979. Statistical and structural approaches to texture. Proceedings of the IEEE 67 (5), 786–804.

Hill, R.A., Boyd, D.S., Hopkinson, C., 2011. Relationship between canopy height and Landsat ETM+ response in lowland Amazonian rainforest. Remote Sensing Letters 2 (3), 203–212.

Houghton, R.A., Skole, D.L., Nobre, C.A., Hackler, J.L., Lawrence, K.T., Chomentowski, W.H., 2000. Annual fluxes of carbon from deforestation and regrowth in the Brazilian Amazon. Nature 403 (6767), 301–304.

Hyde, P., Dubayah, R., Walker, W., Blair, B., Hofton, M., Hunsaker, C., 2006. Mapping forest structure for wildlife habitat analysis using multi-sensor (LiDAR, SAR/InSAR, ETM+, Quickbird) synergy. Remote Sensing of Environment 102 (1–2), 63–73.

Imhoff, M.L., 1995. Radar backscatter and biomass saturation: ramifications for global biomass inventory. IEEE Transactions of Geoscience and Remote Sensing 33 (2), 511–518.

Kellndorfer, J., Pierce, L.E., Dobson, M.C., Ulaby, F.T., 1998. Toward consistent regional-to-global-scale vegetation characterisation using orbital SAR systems. IEEE Transactions of Geoscience and Remote Sensing 36 (5), 1396–1411.

Kuplich, T.M., Curran, P.J., Atkinson, P.M., 2005. Relating SAR image texture to biomass of regenerating tropical forests. International Journal of Remote Sensing 26 (21), 4829–4854.

Le Toan, T., Beaudoin, A., Riom, J., Guyon, D., 1992. Relating forest biomass to SAR data. IEEE Transactions on Geoscience and Remote Sensing 30 (2), 390–402.

Lu, D., Batistella, M., 2005. Exploring TM image texture and its relationships with biomass estimation in Rondônia, Brazilian Amazon. Acta Amazonica 35 (2), 249–257.

Lu, D., 2006. The potential and challenge of remote sensing-based biomass estimation. International Journal of Remote Sensing 27 (7), 1297–1328.

Lucas, R.M., Honzak, M., do Amaral, I., Curran, P.J., Foody, G.M., 2002. Forest regeneration on abandoned clearances in central Amazonia. International Journal of Remote Sensing 23 (5), 965–988.

Lucas, R.M., Cronin, N., Lee, A., Moghaddam, M., Witte, C., Tickle, P., 2006a. Empirical relationships between AIRSAR backscatter and LiDAR-derived forest biomass, Queensland, Australia. Remote Sensing of Environment 100 (3), 407–425.

Lucas, R.M., Cronin, N., Moghaddam, M., Lee, A., Armston, J., Bunting, P., Witte, C., 2006b. Integration of radar and Landsat-derived foliage projected cover for woody regrowth mapping, Queensland, Australia. Remote Sensing of Environment 100 (3), 388–406.

Luckman, A., Baker, J.R., Kuplich, T.M., Yanasse, C.C.F., Frery, A.C., 1997. A study of the relationship between radar backscatter and regenerating forest biomass for spaceborne SAR instruments. Remote Sensing of Environment 60 (1), 1–13.

Malhi, Y., 2010. The carbon balance of tropical forest regions, 1990–2005. Current Opinion in Environmental Sustainability 2 (4), 237–244.

Mitchard, E.T.A., Saatchi, S.S., Woodhouse, I.H., Nangendo, G., Ribeiro, N.S., Williams, M., Ryan, C.M., Lewis, S.L., Feldpausch, T.R., Meir, P., 2009. Using satellite radar backscatter to predict above-ground biomass: a consistent relationship across four different African landscapes. Geophysical Research Letters 36, L243401. http://dx.doi.org/10.1029/2009GL040692.

Nagendra, H., 2001. Using remote sensing to assess biodiversity. International Journal of Remote Sensing 22 (12), 2377–2400.

Newbery, D.M., Campbell, E.J.F., Lee, Y.F., Ridsdale, C.E., Still, M.J., 1992. Primary lowland dipterocarp forest at Danum Valley. Philosophical Transactions of the Royal Society B 335 (1275), 341–356.

Pelz, D.R., 2000. Forest inventories in tropical forests in S.E. Asia (Thailand and Malaysia). Proc. of Taller Internacional de Evaluacion y Monitoreo en Bosques Tropicales 2000. Guadajera, Mexico.

Podest, E., Saatchi, S., 2002. Application of multiscale texture in classifying JERS-1 radar data over tropical vegetation. International Journal of Remote Sensing 23 (7), 1487–1506.

Rauste, Y., 2005. Multi-temporal JERS SAR data in boreal forest mapping. Remote Sensing of Environment 97 (2), 263–275.

Shimada, M., 2002. User's Guide to NASDA's SAR products (Version 3). NASDA, NDX000291.

Simard, M., De Grandi, G., Thomson, K.P.B., 1998. Adaption of the wavelet transform for the construction of multiscale texture maps of SAR images. Canadian Journal of Remote Sensing 24, 264–285.

Simard, M., Saatchi, S.S., De Grandi, G., 2000. The use of decision tree and multiscale texture for classification of JERS-1 SAR data over tropical forest. IEEE Transactions on Geoscience and Remote Sensing 38 (5), 2310–2321.

Steininger, M.K., 2000. Satellite estimation of tropical secondary forest aboveground biomass data from Brazil and Bolivia. International Journal of Remote Sensing 21 (6–7), 1139–1157.

Sun, G., Ranson, K.J., Kharuk, V.I., 2002. Radiometric slope correction for forest biomass estimation from SAR data in the Western Sayani Mountains, Siberia. Remote Sensing of Environment 79 (2–3), 279–287.

Uhl, C., Buschbacher, R., Serrao, E.A.S., 1988. Abandoned pastures in Eastern Amazonia. I. Patterns of plant succession. Journal of Ecology 76 (3), 663–681.

UN-REDD, 2008, *Role of satellite remote sensing in REDD*, UN-REDD Programme Working Paper 1, available at: http://www.un-redd.org/Publications/.

Wang, C., Qi, J., 2008. Biophysical estimation in tropical forests using JERS-1 SAR and VNIR imagery: II. Above ground woody biomass. International Journal of Remote Sensing 29 (23), 6827–6849.

Wilkinson, G.G., 1997. Open Questions in Neurocomputing for Earth Observation. In: Kanellopoulos, I., Wilkinson, G.G., Rolli, F., Austin, J. (Eds.), Neurocomputing in Remote Sensing Data Analysis. Springer, Berlin.

Woodcock, C.E., Macomber, S.A., Pax-Lenney, M., Cohen, W.B., 2001. Monitoring large areas for forest change using Landsat: generalisation across space, time and Landsat sensors. Remote Sensing of Environment 78 (1–2), 194–203.

Woodcock, C.E., 2002. Uncertainty in Remote Sensing. In: Foody, G.M., Atkinson, P.M. (Eds.), Uncertainty in Remote Sensing and GIS. Wiley, Chichester.